Reliability-Constrained Optimal Scheduling of Interconnected Microgrids

Abdullah Albaker

Department of Electrical Engineering, College of Engineering, University of Ha'il, Saudi Arabia
af.albaker@uoh.edu.sa (corresponding author)

ABSTRACT

This paper proposes a Mixed-Integer Linear Programming (MILP) optimization model for the scheduling problem of the interconnected microgrid system. The proposed model is capable of efficiently minimizing the microgrids' total operating costs and improving the entire system's reliability, as it is constrained based on enhancing the interconnected microgrids' reliability. The Expected Energy Not Supplied (*EENS*) is considered in order to ensure minimizing the interconnected microgrids' power deficiency. Furthermore, the proposed model has the capability to solve the optimization problem considering the islanded operation of the interconnected microgrids, i.e. when disturbances occur on the upstream grid. Numerical simulations on a test system containing three interconnected microgrids are performed to evaluate the effectiveness of the model and the results demonstrate the merits and features of the reliability-constrained optimal scheduling model in minimizing the interconnected microgrids' total operating costs and enhancing the interconnected system reliability.

Keywords-distributed energy resources; Expected Energy Not Supplied (EENS); interconnected microgrids; islanded operation; optimization; optimal scheduling

I.   INTRODUCTION

The reliability of power systems is one of the most important factors of human quality of life, as power outages for a few minutes may cause serious problems [1-4]. Therefore, it is significant to constantly develop and improve the reliability of power systems in order to maintain their quality and sustainability [5-8]. Enhancing and evaluating the power systems' reliability has been extensively researched and analyzed. Authors in [9] investigated the reliability analysis of the IEEE40-bus system coupled with enormous PV and wind systems. By dividing the power system layout into various parts, the zone branch approach was used to evaluate the reliability parameters of the distribution systems. In [10], a cost-reliability bi-objective optimization model was developed for microgrids to acquire the optimal sizing and sitting of energy storage systems. The developed model included minimizing the microgrid's total cost and Loss Of Load Expectation (LOLE) and the ε-constraint method and fuzzy satisfying technique were utilized to solve the proposed problem. The uncertainty related to the availability of capacity and the load level was taken into consideration in [11] using a generic and coherent approach. In addition, applications were illustrated and a new method for the determination of the probabilistic assessment of reliability indices and performance quality metrics was described. In [12], a comprehensive methodological framework was proposed, based on quantitative and Latin hypercube sampling methods, to study the prospective impact of vehicle-to-grid with utility-connected battery swapping station for enhancing the supply dependability in future distribution networks. The study in [13]

utilizes the fmincon optimization tool to inspect the impact of integrating renewable energy resources into microgrids in terms of measuring and evaluating the enhancement of the system's reliability. The obtained results indicated the improvement of measuring the system's reliability. Authors in [14] proposed an optimization model based on enhancing the reliability to solve the optimal scheduling problem of the integrated microgrids and evaluated some of the reliability indices of the system including CAIDI, SAIDI, and SAIFI. Microgrids as an intelligent technique are partially intended to support power systems' reliability [15-18].

Microgrids are typically designed to facilitate integrating Distributed Energy Resources (DERs) into power systems to support the local load demand and expand the predicted economic benefits [19-21]. DERs may involve non-dispatchable renewable units, Battery Energy Storage Systems (BESSs), and dispatchable Distributed Generators (DGs) [22-24]. Once the microgrids are developed, achieving optimal scheduling is a crucial factor in realizing the desired objectives. Several research studies have been extensively conducted in this field [25-31]. In [25], an optimization resiliency-oriented scheduling model was proposed to enhance the resiliency of the microgrid by reducing local load curtailment. Authors in [26], proposed an optimization model to solve the scheduling problem of several integrated microgrids using the Lagrangian relaxation method to preserve the microgrids' privacy. In [27], a discretized step transformation scheme based on chance-constrained programming was proposed considering the spinning reserve uncertainty to solve the scheduling problem for isolated microgrids. Authors in [28] proposed an optimal

scheduling strategy to regulate the microgrid operation and support its resiliency based on developed constraints that enable the islanding operation. Authors in [29] proposed a multi-objective optimization approach to determine the optimal scheduling of unbalanced microgrids considering energy saving, improvement of power quality, and cost minimization. In [30], an automated reinforcement learning-based optimization scheme was proposed considering multi-period forecasting associated with load and renewable generation to solve the optimal scheduling problem of isolated microgrids. Authors in [31] proposed a scheduling model considering radiation changes of photovoltaic systems and uncertainties associated with grid bid changes and load demand forecasting to solve the optimization problem. In addition, they utilized a modified bat algorithm to solve the proposed problem considering a variety of uncertainties. Nonetheless, the microgrids can be interconnected to each other to maximize the anticipated goals. The optimal interconnected operation of the microgrids can maximize the reliability and resiliency of local power systems, boost the economic advantages of individual microgrids, and foster the use of renewable energy resources.

The current paper proposes a generic optimization model to solve the optimal scheduling problem of interconnected microgrids considering enhancing the interconnected system's reliability. Based on the developed operational constraints, the proposed model minimizes each microgrid's Expected Energy Not Supplied (*EENS*), hence, maximizing the reliability of each microgrid involved in the system. In addition, it minimizes the entire interconnected system's total operation cost. Furthermore, it is featured with the capability to solve the scheduling optimization problem during the islanded operation. The proposed optimization problem is developed based on a Mixed Integer Linear Programming (MILP) and solved over a completed 24-hour scheduling horizon.

II. MODEL OUTLINE

The proposed reliability-constrained optimal scheduling model of interconnected microgrids aims to minimize each microgrid's "involved in the integrated system" total operation cost and minimize the microgrid's *EENS*. In addition, it considers the optimal scheduling of the interconnected microgrids during both grid-connected and islanded operations, i.e. during outages and disturbances.

The microgrids will exchange the power (export and import) with the utility grid during the grid-connected mode to maximize their economic benefits, while they exchange power locally, i.e. among the interconnected microgrids, during the islanded mode to boost and maximize their reliability and own economic benefits. To clarify this significant point, there will be no local power exchange among the interconnected microgrids during the grid-connected mode since it will be more economical for the seller microgrid to sell its excess generation to the utility rather than the other interconnected microgrids. On the other side, the microgrid that experiences a power deficiency would prefer to buy the power from the utility, as they have the option to buy their further needs of power at cheaper prices at the hourly market prices. Accordingly, there is no power exchange among the interconnected microgrids during the grid-connected mode,

while they will observably exchange power during the islanded operation for mutual benefits, i.e. to increase the seller microgrids' economic benefits and minimize the buyer microgrids' energy deficiency.

The proposed interconnected microgrid system is demonstrated in Figure 1. It is worth mentioning that the developed model would significantly improve the individual microgrid's reliability in addition to the overall reliability of the interconnected system as it pointedly encourages the microgrids to exploit all available DERs of the interconnected system as much as possible. In other words, the proposed model inspires the microgrids to exploit all installed DERs to supply the other microgrids that experience power deficiencies for mutual benefit.
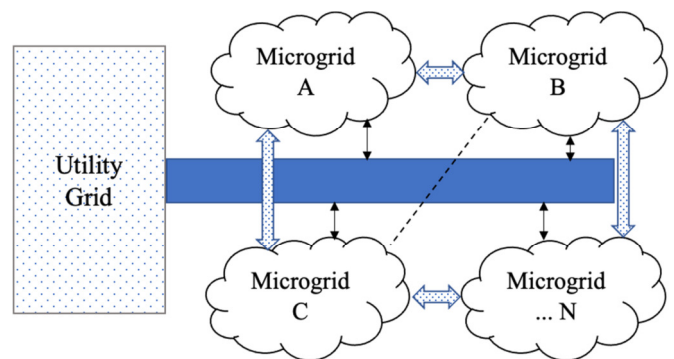

Fig. 1.   Interconnected microgrid system.

III. PROBLEM FORMULATION

The objective function of the proposed reliability-constrained optimal scheduling problem of the interconnected microgrid system aims to minimize each microgrid's total operating costs and to minimize the probability of power deficiency occurrences within the microgrids, as follows:

$$\min \sum_t^T \sum_m^M \sum_s^K \left(\sum_i^G F_{mi}\,(P_{tmsi})\,I_{tmi} + \rho_{tm} P_{tms}^M + \sum_{n,n\neq m}^M \lambda_{tmn} P_{tmns}^C - \kappa\,PD_{tms} \right) \tag{1}$$

The developed objective function involves four main expressions. The first expression represents the generated power from the installed dispatchable DERs, which is further multiplied by a commitment binary indicator to specify the commitment state. The second expression represents exchanging the power with the utility grid. Nonetheless, this expression could mean either cost or revenue depending on the power flow direction. The third expression represents the power exchange between the interconnected microgrids. However, this expression will bring cost for buyer microgrids and revenue for seller microgrids. The last expression is added to add value to the percentage of the power deficiency within the microgrids. The minus sign is added as the percentage of the power deficiency will be displayed in the negative. Nonetheless, it is multiplied by an auxiliary cost value, which is supposed to be higher than the other costs to prioritize the reliability of the interconnected system. It should be indicated

that the proposed optimization model is developed to be compatible with both, islanded and grid-connected, modes using the islanded operating indicator s.

$$\sum_i^G P_{tmsi} + P_{tms}^R + \sum_i^S P_{tmsi} + P_{tms}^M$$

$$+ \sum_{n, n \neq m}^M P_{tmns}^C = D_{tms} - EENS_{tms} \qquad \forall t, \forall m, \forall s \qquad (2)$$

$$-P^{M, \max} U_{ts} \leq P_{tms}^M \leq P^{M, \max} U_{ts} \qquad \forall t, \forall m, \forall s \qquad (3)$$

$$-P^{C, \max}\left(1 - U_{ts}\right) \leq P_{tms}^C \leq P^{C, \max}\left(1 - U_{ts}\right) \qquad \forall t, \forall m, \forall s \qquad (4)$$

The total generated and imported power must be balanced with the total power demand, which is satisfied by (2). However, it is worth mentioning that the *EENS* is included in the power balance equation to achieve a feasible solution during outages or disturbances, i.e. during the islanded operation. The power exchange between the microgrids and the utility grid must be within the maximum line capacity limits, which is satisfied by (3). Nonetheless, the line capacity limits are multiplied by the islanding binary variable to regulate the microgrids' operating modes among the islanded and grid-connected operation. On the other side, the power exchange among the interconnected microgrids is also subjected to line capacity limits, which is satisfied by (4). However, it should be mentioned that this operational constraint is also multiplied by the islanding binary variable to force the power exchange between the interconnected microgrids to zero during the grid-connected operation.

$$P_{mi}^{\min} I_{tmi} \leq P_{tmsi} \leq P_{mi}^{\max} I_{tmi} \qquad \forall t, \forall m, \forall s, \forall i \in G \qquad (5)$$

$$P_{tmsi} - P_{(t-1)msi} \leq UR_i \qquad \forall t, \forall m, \forall s, \forall i \in G \qquad (6)$$

$$P_{(t-1)msi} - P_{tmsi} \leq DR_{mi} \qquad \forall t, \forall m, \forall s, \forall i \in G \qquad (7)$$

$$T_{mi}^{on} \geq UT_{mi}\left(I_{tmi} - I_{(t-1)mi}\right) \qquad \forall t, \forall m, s=0, \forall i \in G \qquad (8)$$

$$T_{mi}^{off} \geq DT_{mi}\left(I_{(t-1)mi} - I_{tmi}\right) \qquad \forall t, \forall m, s=0, \forall i \in G \qquad (9)$$

The installed dispatchable units are subject to respective operational constraints to regulate their operation. Each dispatchable unit can generate power only between the maximum and minimum capacity limits, which are satisfied by (5). In addition, they are multiplied by a commitment binary variable I to state whether the dispatchable unit is committed or not during the specified optimal scheduling hour. Moreover, each dispatchable unit is restricted by the ramping up and down rate limits, as in (6) and (7), respectively. Furthermore, once the dispatchable unit is switched ON or OFF, it is restricted by the minimum up and down time limits, of (8) and (9), respectively.

$$D_{md}^{\min} z_{tmsd} \leq D_{tmsd} \leq D_{md}^{\max} z_{tmsd} \qquad \forall t, \forall m, \forall s, \forall d \in D_A \qquad (10)$$

$$\sum_{[\alpha_d, \beta_d]} D_{tmsd} = E_{md} \qquad \forall m, \forall s, \forall d \in D_A \qquad (11)$$

$$T_{md}^{on} \geq MU_{md}\left(z_{tmsd} - z_{(t-1)msd}\right) \qquad \forall t, \forall m, s=0, \forall d \in D_A \qquad (12)$$

The adjustable loads are regulated by constraints (10)-(12). Each adjustable load in the microgrids is restricted by the

minimum and maximum rated power, as in (10). However, some of the adjustable loads that are switched ON might be subject to a minimum required energy to accomplish the operating cycle, which is regulated by (11). On the other hand, some adjustable loads must operate continuously for a certain amount of time after being turned ON, which is satisfied by (12).

$$P_{tmsi} \leq P_{tmi}^{dch, \max} u_{tmi} - P_{tmi}^{ch, \min} v_{tmi} \qquad \forall t, \forall m, \forall s, \forall i \in S \qquad (13)$$

$$P_{tmsi} \geq P_{tmi}^{dch, \min} u_{tmi} - P_{tmi}^{ch, \max} v_{tmi} \qquad \forall t, \forall m, \forall s, \forall i \in S \qquad (14)$$

$$C_{tmsi} = C_{(t-1)msi} - P_{tmsi} u_{tmsi} \tau / \eta_i$$
$$- P_{tmsi} v_{tmsi} \tau \qquad \forall t, \forall m, \forall s, \forall i \in S \qquad (15)$$

$$C_{mi}^{\min} \leq C_{tmsi} \leq C_{mi}^{\max} \qquad \forall t, \forall m, \forall s, \forall i \in S \qquad (16)$$

$$T_{mi}^{ch} \geq MC_{mi}\left(u_{tmsi} - u_{(t-1)msi}\right) \qquad \forall t, \forall m, s=0, \forall i \in S \qquad (17)$$

$$T_{mi}^{dch} \leq MD_{mi}\left(v_{tmsi} - v_{(t-1)msi}\right) \qquad \forall t, \forall m, s=0, \forall i \in S \qquad (18)$$

$$u_{tmsi} + v_{tmsi} \leq 1 \qquad \forall t, \forall m, s=0, \forall i \in S \qquad (19)$$

The connected BESSs are subject to several operational constraints to acquire their optimal scheduling. Maximum and minimum charging and discharging restrictions apply to BESSs, as in (13) and (14). In accordance with the charging and discharging operations over the defined scheduling horizon, and taking into account the BESS efficiency, the stored energy in the BESS is calculated by (15). The minimum and maximum capacity restrictions impose additional limits on the BESSs, as in (16). Each BESS is restricted by time limits once it starts charging or discharging, as in (17) and (18), respectively. Furthermore, the binary variables u and v are added to the BESS operational constraints (19) to regulate their operation mode to either charge or discharge during the specified optimal scheduling time.

$$\psi_{tms} = \frac{D_{tms} - EENS_{tms}}{D_{tms}} \qquad \forall t, \forall m, \forall s \qquad (20)$$

$$PD_{tms} = \left(\psi_{tms} - 1\right) \times 100\% \qquad \forall t, \forall m, \forall s \qquad (21)$$

The microgrids' power deficiency is a significant factor in indicating the interconnected microgrids' reliability; thus, it is restricted by the developed constraints (20) and (21). The probability of *EENS* is calculated by (20). The percentage of the microgrids' power deficiency is regulated and measured by (21).

IV. NUMERICAL SIMULATIONS

Three independent microgrids were utilized to study and investigate the proposed reliability-constrained optimal scheduling model of the interconnected microgrids, which are named MG A, MG B, and MG C. The microgrids' local installed dispatchable generators are specified in Table I. The microgrids' BESS characteristics are demonstrated in Table II. The efficiency of all BESS is supposed to be 90% [26]. Each of the microgrids is accompanied with its own renewable, i.e. nondispatchable, generators, and their forecasted power generation is shown in Figures 2 and 3, for solar PVs and wind

turbines power, respectively. Table III shows the characteristics of the adjustable loads that are installed in the microgrids.

TABLE I.   CHARACTERISTICS OF INSTALLED DISPATCHABLE GENERATORS

DG	MG A	MG B	MG C
	Price ($/MWh)		
G 1	28.1	30.9	38.7
G 2	38.9	45.7	46.9
G 3	62.2	73.5	75.4
G 4	66.3	78.4	–
–	**Minimum up and down time (h)**		
G 1	3	4	5
G 2	3	4	4
G 3	1	2	2
G 4	1	3	–
–	**Minimum and maximum capacity (MW)**		
G 1	1 – 5	1 – 2	0.5 – 2
G 2	1 – 5	0.5 – 2	0.8 – 2.5
G 3	0.8 – 3	0.5 – 1	0.5 – 3.5
G 4	0.8 – 3	1 – 3	–
–	**Ramp up and down rate (MW/h)**		
G 1	2.5	1	1.5
G 2	2.5	2	1.5
G 3	3	1	2.5
G 4	3	1.5	–

TABLE II.   MICROGRIDS' BESS CHARACTERISTICS

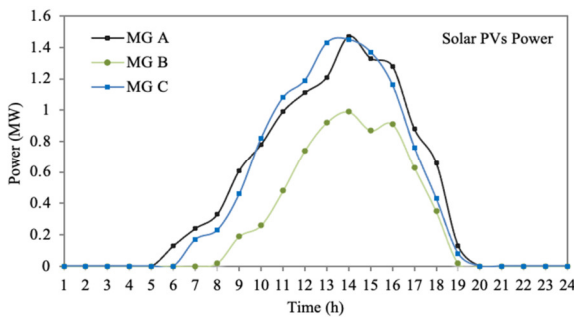| Microgrid	BESS characteristics		
	Charging and discharging minimum and maximum power (MW)	Charging and discharging minimum operating time (h)	Capacity (MWh)
MG A BESS	0.4 – 2	5	10
MG B BESS	0.2 – 1	4	5
MG C BESS	0.8 – 2	4	6

Fig. 2.   Solar PVs power in MG A, MG B, and MG C.

The microgrids' hourly fixed load data are shown in Figure 4. All the microgrids are electrically connected to the utility grid as an infinite bus. The market price of the power exchange between the utility grid and the microgrids is demonstrated in Figure 5. Figure 5 also shows the price of the local power exchange among the interconnected microgrids, which is set to be 10% higher than the market hourly prices arbitrary to create incentive to local power exchanges. In addition, a marginal value of the power deficiency, i.e. κ, of \$10/kWh is assumed [32]. The lines between each microgrid and the utility grid and the lines among the interconnected microgrids are subject to line capacity limits, which are restricted to 10MW and 2MW, respectively. A 24-hour scheduling horizon is considered to solve the proposed problem. In addition, 25-islanded-scenarios

are considered to solve the optimization problem, where one scenario indicates the grid-connected operation and the rest indicate islanded operation in each specific hour. The optimization problem is programmed and solved using CPLEX 11.0 in GAMS [33]. Five case studies were carried out to demonstrate the features and effectiveness of the proposed model. The summary of the microgrids' total operation costs is shown in Table IX for all cases.
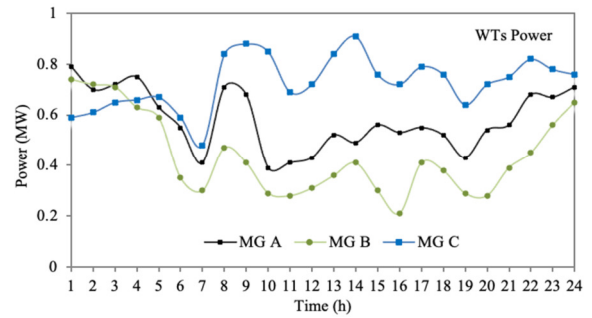

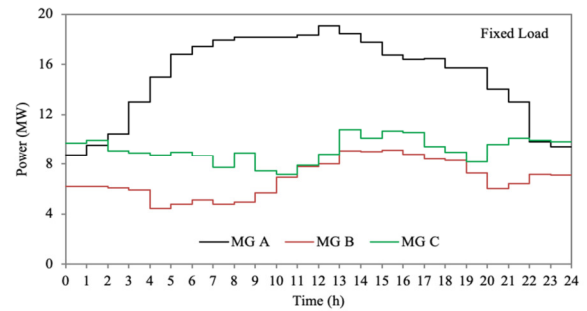Fig. 3.   Wind turbines power in MG A, MG B, and MG C.

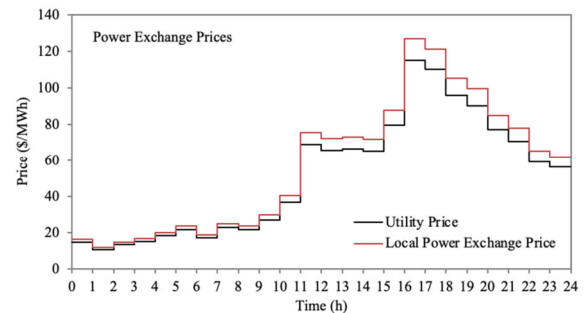Fig. 4.   Hourly fixed load in MG A, MG B, and MG C.

Fig. 5.   Hourly forecasted market prices and local power exchange prices.

A. Case 0-Base Case: Individual Microgrid Optimal Scheduling

In this case, each microgrid in the system is optimized individually, i.e. there is no interconnection among the microgrids, to ensure the lowest potential operational cost and maximum reliability. The total operational costs of MG A, MG B, and MG C, considering the islanded operation scenarios, are computed as \$14,699.19, \$9,387.56, and \$10,001.18, respectively.

TABLE III.   ADJUSTABLE LOAD

| Microgrid	Adjustable load characteristics				
	Load type	Required energy (MWh)	Minimum and maximum capacity (MW)	Start and end time (h)	Minimum up time (h)
MG A	Shiftable 1	1.6	0 – 0.4	11 – 15	1
	Shiftable 2	1.6	0 – 0.4	15 – 19	1
	Shiftable 3	2.4	0.02 – 0.8	16 – 18	1
	Shiftable 4	2.4	0.02 – 0.8	14 – 22	1
	Cuirtailable 5	47	1.8 – 2	1 – 24	24
MG B	Shiftable 1	1.6	0 – 0.4	12 – 16	1
	Shiftable 2	2.4	0.02 – 0.8	15 – 23	1
	Cuirtailable 3	47	1.8 – 2	1 – 24	24
MG C	Shiftable 1	2	0 – 0.5	9 – 13	1
	Shiftable 2	2.4	0.2 – 0.8	11 – 17	1
	Cuirtailable 3	36	0.8 – 1.6	1 – 24	24
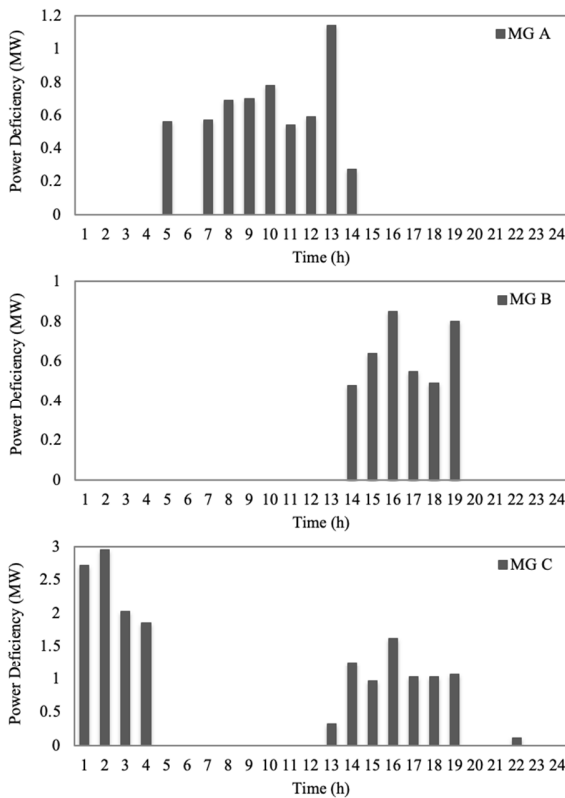
Fig. 6.   Microgrids' power deficiency in Case 0.

In this case, each of the microgrids in the system experiences some power deficiency during the optimal islanded operation, which is illustrated in Figure 6. The percentage of the power deficiency in the microgrids is calculated as 1.61%, 2.33%, and 7.67% for MG A, MG B, and MG C, respectively (see Table VIII). The hourly optimal scheduling of the installed BESSs in the microgrids is demonstrated in Figure 7. This case study demonstrates that although optimal solutions for microgrids are identified, the lack of complementary power supplies may result in failure to reach maximum reliability.

B. Case 1: Optimal Scheduling when the Interconnection is only between MG A and MG B

In this case, the impact of integrating MG A and MG B on the optimization outcomes is investigated. MG A's total operation cost is slightly reduced by 0.34% to $14,648.59,

while the total operation cost of MG B is slightly increased by 0.43% as it is computed to $9,428.60. It should be mentioned that the optimization outcomes of MG C are not impacted in this case study as its optimal scheduling results remained exactly the same as in the base case.
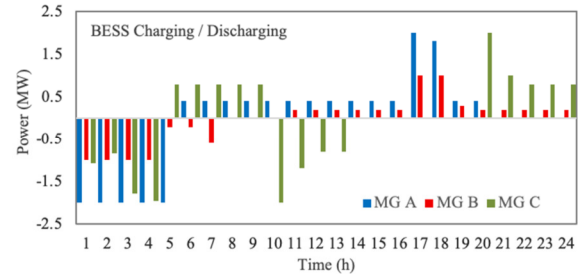

Fig. 7.   Optimal scheduling of the BESS in Case 0.

TABLE IV.   LOCAL POWER EXCHANGE BETWEEN MG A AND MG B IN CASE 1

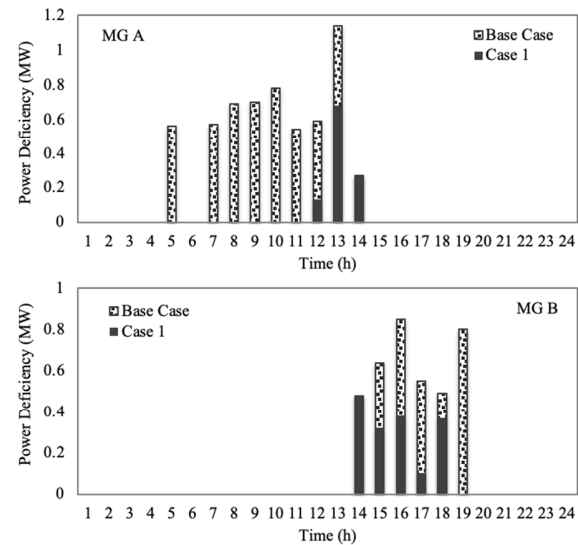| Scenario no.	1	2	3	4	5	6	7	8
$P^{C(A-B)}$ (MW)	–0.26	–0.47	–0.36	–0.28	0.56	0	0.57	0.69
Scenario no.	9	10	11	12	13	14	15	16
$P^{C(A-B)}$ (MW)	0.70	0.78	0.54	0.46	0.46	0	–0.32	–0.47
Scenario no.	17	18	19	20	21	22	23	24
$P^{C(A-B)}$ (MW)	–0.45	–0.12	–0.80	0	0	0	0	0

Fig. 8.   Power deficiency differences in Case 1 for MG A and MG B.

The hourly power deficiency is reduced by 81.98% and 56.65% for MG A and MG B, respectively, as shown in Figure 8. In this case, MG A and MG B experience power deficiency of 0.29% and 1.01%, respectively. The percentage of power deficiency is summarized in Table VIII for all cases. Obviously, enabling the integration among these two microgrids would result in permitting local power exchange among them. The results of the optimal hourly power exchange among the interconnected microgrids are shown in Table IV. It should be noted that the minus sign signifies that the power is transferred from MG A to MG B, and vice versa. Observably, allowing the integration among certain microgrids

demonstrates slight improvements in terms of interconnected microgrids' economic benefits and improves their reliability as it authorizes further paths to optimize the microgrid scheduling.

C. Case 2: Optimal Scheduling when the Interconnection is only between MG A and MG C

In this case study, the interconnection among the interconnected microgrids is only enabled between MG A and MG C. The microgrids' total operation cost is computed as $14,201.05 and $10,569.53 for MG A and MG C, respectively, while the total operating cost of MG B remained unchanged as in case 0. Even though the total operation cost of MG C is increased by 5.68%, the power deficiency of MG C is obviously reduced by 87.39%. The percentage of the power deficiency is computed as 0.22% and 0.97% for MG A and MG C, respectively, while it remained unchanged for MG B, as shown in Table VIII.

TABLE V. LOCAL POWER EXCHANGE BETWEEN MG A AND MG C IN CASE 2

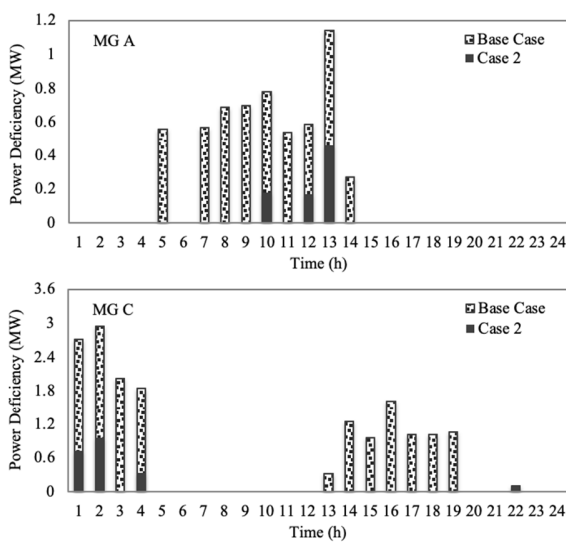| Scenario no.	1	2	3	4	5	6	7	8
$P^{C(A-C)}$ (MW)	−2	−2	−2	−1.52	0.56	0	0.57	0.69
Scenario no.	9	10	11	12	13	14	15	16
$P^{C(A-C)}$ (MW)	0.70	0.60	0.54	0.42	0.68	0.29	0	0
Scenario no.	17	18	19	20	21	22	23	24
$P^{C(A-C)}$ (MW)	0	0	−1.06	−0.25	−1.66	−2	−1.94	−1.89

Fig. 9. Power deficiency differences in Case 2 for MG A and MG C.

The hourly power exchange between MG A and MG C is illustrated in Table V. The minus sign indicates that the power is transferred from MG A to MG C, and vice versa. The improvements in the microgrids' power deficiency are graphically illustrated in Figure 9, which also shows the hourly load curtailment in MG A and MG C.

D. Case 3: Optimal Scheduling when the Interconnection is only between MG B and MG C

In this case, the interconnection among MG B and MG C is activated, hence, the power can be locally exchanged among these interconnected microgrids. The optimization results of the

hourly local power exchange are illustrated in Table VI, where the minus sign indicates that the power is exported from MG B to MG C and vice versa. The total operating costs of these two interconnected microgrids are slightly changed, as it is indicated in Table IX. MG B's total operating cost is reduced by 0.61% (computed as $9,329.68), while MG C's total operating cost is slightly increased by 1.19% (computed as $10,120.02). However, the power deficiency of these two microgrids is noticeably decreased, by 65.23% and 58.15% for MG B and MG C, respectively. The changes in the power deficiency are graphically demonstrated in Figure 10. The reduction percentage of total power deficiency is calculated as 0.81% and 3.21% for MG B and MG C, respectively, as it is shown in Table VIII. On the other side, the optimization results of MG A have not been changed compared with the base case, as it is excluded in this case study from the interconnection.

TABLE VI. LOCAL POWER EXCHANGE BETWEEN MG B AND MG C IN CASE 3

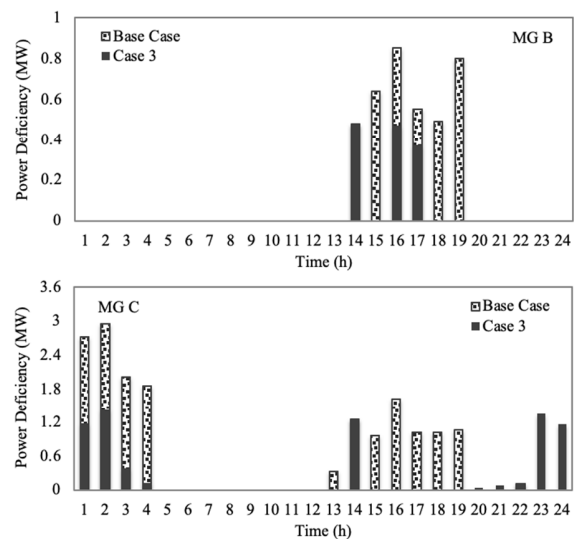| Scenario no.	1	2	3	4	5	6	7	8
$P^{C(B-C)}$ (MW)	−0.74	−0.73	−0.84	−0.92	−0.90	−1.19	−0.84	−0.28
Scenario no.	9	10	11	12	13	14	15	16
$P^{C(B-C)}$ (MW)	−1.19	0	0	0	0	0	0.66	0.38
Scenario no.	17	18	19	20	21	22	23	24
$P^{C(B-C)}$ (MW)	0.18	0.51	0.82	−0.21	−1.58	−1.22	−0.59	−0.73

Fig. 10. Power deficiency differences in Case 3 for MG B and MG C.

E. Case 4: Optimal Interconnected Microgrids Scheduling

In this case, all microgrids are electrically interconnected in the studied system. This case study inspects and explores the potential impacts of interconnecting the microgrids on their total operating costs and reliability. The optimal local power exchange scheduling among the interconnected microgrids, over the scheduling horizon, is demonstrated in Table VII. The optimization results of the optimal scheduling of the BESS are slightly changed in this case study, which is demonstrated in Figure 11. These slight changes are caused by the local power exchange among the microgrids. The total operating costs of the interconnected microgrids are computed as $14,379.87, $9,328.19, and $10,308.36 for MG A, MG B, and MG C,

respectively. Even though the total operating costs are slightly increased in some of the microgrids (by 3.07% in MG C), the encountered power deficiency in all the microgrids is dramatically minimized to zero, which emphasizes a significant improvement in the interconnected system reliability.

TABLE VII.   LOCAL POWER EXCHANGE BETWEEN ALL THE MICROGRIDS IN CASE 4

Scenario no.	1	2	3	4	5	6	7	8
$P^{C(A\text{-}B)}$ (MW)	−1.18	−1.42	−0.38	0	0.56	0	0.57	0.37
$P^{C(A\text{-}C)}$ (MW)	−2	−2	−2	−1.13	0	0	0	0.32
$P^{C(B\text{-}C)}$ (MW)	−0.72	−0.95	−0.02	−0.72	−0.90	−1.19	−0.84	0
Scenario no.	9	10	11	12	13	14	15	16
$P^{C(A\text{-}B)}$ (MW)	0.70	0	0	0.17	0.46	0	−0.22	−0.47
$P^{C(A\text{-}C)}$ (MW)	0	0.78	0.54	0.42	0.68	0.27	0	0
$P^{C(B\text{-}C)}$ (MW)	−0.39	0	0	0	0	0.48	0.44	0.38
Scenario no.	17	18	19	20	21	22	23	24
$P^{C(A\text{-}B)}$ (MW)	−0.45	−0.01	−0.80	0	0	0	0	0
$P^{C(A\text{-}C)}$ (MW)	0	0	−0.26	−0.04	−0.10	−0.91	−1.85	−1.66
$P^{C(B\text{-}C)}$ (MW)	0.10	0.48	0	−0.21	−1.56	−1.20	−0.90	−0.23

TABLE VIII.   PERCENTAGE OF MICROGRIDS' POWER DEFICIENCY IN ALL CASE STUDIES

Case no.	MG A	MG B	MG C
Case 0	1.61%	2.33%	7.67%
Case 1	0.29%	1.01%	7.67%
Case 2	0.22%	2.33%	0.97%
Case 3	1.61%	0.81%	3.21%
Case 4	0%	0%	0%

TABLE IX.   SUMMARY OF MICROGRIDS' TOTAL OPERATION COST

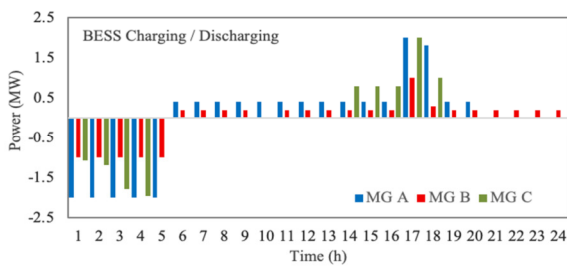| Case no.	MG A	MG B	MG C
Case 0	$14,699.19	$9,387.56	$10,001.18
Case 1	$14,648.59	$9,428.60	$10,001.18
Case 2	$14,201.05	$9,387.56	$10,569.53
Case 3	$14,699.19	$9,329.68	$10,120.02
Case 4	$14,379.87	$9,328.19	$10,308.36

Fig. 11.   Optimal scheduling of the BESS in Case 4.

V.   CONCLUSION

This paper highlighted the potential benefits and features of enabling the interconnection among adjacent microgrids and proposed a reliability-constrained optimal scheduling model for interconnected microgrids. The proposed model was capable of economically minimizing the interconnected microgrids' total operating costs and was capable of efficiently maximizing the interconnected system's reliability. The key features of the proposed optimization model can be summarized as follows: (i) it ensures the minimization of the microgrids' total operating costs and supports the optimization of the battery energy storage systems scheduling, (ii) it is capable of efficiently

maximizing the interconnected system reliability by minimizing the expected energy not supplied in the microgrids, (iii) it takes the potentiality of islanded operation scenarios into account (i.e. in the event of disturbances and outages), and (iv) it is developed based on mixed-integer linear programming to facilitate reaching fast and efficient optimal solutions.

The proposed model exploited all the distributed energy resources installed in the microgrids, including the battery energy storage systems, to support the reliability and economic benefits of the microgrids by enabling local power exchange among the interconnected system. The proposed optimization scheme was investigated in several case studies, including the optimal individual scheduling of the microgrids as a base case, to explore and validate its performance and feasibility. The obtained optimization results indicated its superior performance in minimizing the microgrids' total operating costs and the expected energy not supplied in the microgrids. Nevertheless, the proposed optimization model is generic, and various test systems could be applied to investigate its feasibility and performance without loss of generality.

NOMENCLATURE

Indices:

ch	Superscript for BESS charging operation mode.
d	Index for loads.
dch	Superscript for BESS discharging operation mode.
i	Index for DERs.
s	Index for scenarios.
m,n	Index for microgrids.
t	Index for time.

Sets:

D_A	Set of adjustable loads.
G	Set of dispatchable generators.
M	Set of microgrids.
K	Set of islanded scenarios.
S	Set of BESSs.
T	Set of time periods.

Parameters:

DR	Ramping down rate.
D	Aggregated load demand.
DT	Minimum down time.
D^{max}	Adjustable load maximum rated power.
D^{min}	Adjustable load minimum rated power.
E	Total required energy of adjustable load.
$F(.)$	Generation cost of DERs.
MC	Minimum charging time of BESS.
MD	Minimum discharging time of BESS.
MU	Minimum operation time of adjustable load.
P^R	Aggregated forecasted renewable generation.
UR	Ramping up rate.
UT	Minimum up time.
ρ	Forecasted hourly market prices.
κ	Value of power deficiency.
λ	Local power exchange prices.
α, β	Adjustable loads' defined start and end times.
η	BESS efficiency.

Variables:

C	Total stored energy in BESS.
$EENS$	Expected energy not supplied.
I	Binary variable for commitment status of dispatchable units.
P	DERs generated power.
P^C	Local power exchange.
PD	Power deficiency.
P^M	Power exchange with the utility.
T^{ch}	BESS's number of successive charging hours.

T^{dch}	BESS's number of successive discharging hours.
T^{on}	Total number of successive ON hours.
T^{off}	Total number of successive OFF hours.
U	Binary variable for islanding operation status.
τ	Time period.
u	Discharging state of BESS.
v	Charging state of BESS.
ψ	Probability of expected energy not supplied.
z	Adjustable load status.

REFERENCES

[1] M. Koroglu, B. R. Irwin, and K. A. Grepin, "Effect of power outages on the use of maternal health services: evidence from Maharashtra, India," *BMJ Global Health*, vol. 4, no. 3, Jun. 2019, Art. no. e001372, https://doi.org/10.1136/bmjgh-2018-001372.

[2] S. Peyghami, P. Palensky, and F. Blaabjerg, "An Overview on the Reliability of Modern Power Electronic Based Power Systems," *IEEE Open Journal of Power Electronics*, vol. 1, pp. 34–50, 2020, https://doi.org/10.1109/OJPEL.2020.2973926.

[3] M. Shuai, W. Chengzhi, Y. Shiwen, G. Hao, Y. Jufang, and H. Hui, "Review on Economic Loss Assessment of Power Outages," *Procedia Computer Science*, vol. 130, pp. 1158–1163, Jan. 2018, https://doi.org/10.1016/j.procs.2018.04.151.

[4] B. A. Apenteng, S. T. Opoku, D. Ansong, E. A. Akowuah, and E. Afriyie-Gyawu, "The effect of power outages on in-facility mortality in healthcare facilities: Evidence from Ghana," *Global Public Health*, vol. 13, no. 5, pp. 545–555, May 2018, https://doi.org/10.1080/17441692.2016.1217031.

[5] J. Aghaei, M.-I. Alizadeh, P. Siano, and A. Heidari, "Contribution of emergency demand response programs in power system reliability," *Energy*, vol. 103, pp. 688–696, May 2016, https://doi.org/10.1016/j.energy.2016.03.031.

[6] M. Fan, K. Sun, D. Lane, W. Gu, Z. Li, and F. Zhang, "A Novel Generation Rescheduling Algorithm to Improve Power System Reliability With High Renewable Energy Penetration," *IEEE Transactions on Power Systems*, vol. 33, no. 3, pp. 3349–3357, Feb. 2018, https://doi.org/10.1109/TPWRS.2018.2810642.

[7] P. Zhou, R. Y. Jin, and L. W. Fan, "Reliability and economic evaluation of power system with renewables: A review," *Renewable and Sustainable Energy Reviews*, vol. 58, pp. 537–547, May 2016, https://doi.org/10.1016/j.rser.2015.12.344.

[8] Y. Bao, C. Guo, J. Zhang, J. Wu, S. Pang, and Z. Zhang, "Impact analysis of human factors on power system operation reliability," *Journal of Modern Power Systems and Clean Energy*, vol. 6, no. 1, pp. 27–39, Jan. 2018, https://doi.org/10.1007/s40565-016-0231-6.

[9] S. M. Ghania, K. R. M. Mahmoud, and A. M. Hashmi, "A Reliability Study of Renewable Energy Resources and their Integration with Utility Grids," *Engineering, Technology & Applied Science Research*, vol. 12, no. 5, pp. 9078–9086, Oct. 2022, https://doi.org/10.48084/etasr.5090.

[10] S. Nojavan, M. Majidi, and N. N. Esfetanaj, "An efficient cost-reliability optimization model for optimal siting and sizing of energy storage system in a microgrid in the presence of responsible load management," *Energy*, vol. 139, pp. 89–97, Nov. 2017, https://doi.org/10.1016/j.energy.2017.07.148.

[11] B. M. Alshammari, "Probabilistic Evaluation of a Power System's Reliability and Quality Measures," *Engineering, Technology & Applied Science Research*, vol. 10, no. 2, pp. 5570–5575, Apr. 2020, https://doi.org/10.48084/etasr.3441.

[12] B. Zeng, Y. Luo, C. Zhang, and Y. Liu, "Assessing the Impact of an EV Battery Swapping Station on the Reliability of Distribution Systems," *Applied Sciences*, vol. 10, no. 22, Jan. 2020, Art. no. 8023, https://doi.org/10.3390/app10228023.

[13] T. Adefarati and R. C. Bansal, "Reliability and economic assessment of a microgrid power system with the integration of renewable energy resources," *Applied Energy*, vol. 206, pp. 911–933, Nov. 2017, https://doi.org/10.1016/j.apenergy.2017.08.228.

[14] A. Albaker, "Reliability-Based Optimal Integrated Microgrid Scheduling in Distribution Systems," *Engineering, Technology & Applied Science*

[15] *Research*, vol. 13, no. 2, pp. 10395–10400, Apr. 2023, https://doi.org/10.48084/etasr.5727.

[15] M. A. Jirdehi, V. S. Tabar, S. Ghassemzadeh, and S. Tohidi, "Different aspects of microgrid management: A comprehensive review," *Journal of Energy Storage*, vol. 30, Aug. 2020, Art. no. 101457, https://doi.org/10.1016/j.est.2020.101457.

[16] S. Muchande and S. Thale, "Hierarchical Control of a Low Voltage DC Microgrid with Coordinated Power Management Strategies," *Engineering, Technology & Applied Science Research*, vol. 12, no. 1, pp. 8045–8052, Feb. 2022, https://doi.org/10.48084/etasr.4625.

[17] I.-S. Bae and J.-O. Kim, "Reliability Evaluation of Customers in a Microgrid," *IEEE Transactions on Power Systems*, vol. 23, no. 3, pp. 1416–1422, Dec. 2008, https://doi.org/10.1109/TPWRS.2008.926710.

[18] J. C. Lopez, M. Lavorato, and M. J. Rider, "Optimal reconfiguration of electrical distribution systems considering reliability indices improvement," *International Journal of Electrical Power & Energy Systems*, vol. 78, pp. 837–845, Jun. 2016, https://doi.org/10.1016/j.ijepes.2015.12.023.

[19] "Department of Energy." https://www.energy.gov/oe/downloads/%2520 microgrid-workshop-report-august-2011.

[20] B. Kroposki, R. Lasseter, T. Ise, S. Morozumi, S. Papathanassiou, and N. Hatziargyriou, "Making microgrids work," *IEEE Power and Energy Magazine*, vol. 6, no. 3, pp. 40–53, Feb. 2008, https://doi.org/10.1109/MPE.2008.918718.

[21] M. Shahidehpour, "Role of smart microgrid in a perfect power system," in *IEEE PES General Meeting*, Minneapolis, MN, USA, Jul. 2010, pp. 1–1, https://doi.org/10.1109/PES.2010.5590068.

[22] A. Albaker, M. Alturki, R. Abbassi, and K. Alqunun, "Zonal-Based Optimal Microgrids Identification," *Energies*, vol. 15, no. 7, Jan. 2022, Art. no. 2446, https://doi.org/10.3390/en15072446.

[23] A. Khodaei, "Provisional Microgrids," *IEEE Transactions on Smart Grid*, vol. 6, no. 3, pp. 1107–1115, Feb. 2015, https://doi.org/10.1109/TSG.2014.2358885.

[24] K. Gao, T. Wang, C. Han, J. Xie, Y. Ma, and R. Peng, "A Review of Optimization of Microgrid Operation," *Energies*, vol. 14, no. 10, Jan. 2021, Art. no. 2842, https://doi.org/10.3390/en14102842.

[25] A. Khodaei, "Resiliency-Oriented Microgrid Optimal Scheduling," *IEEE Transactions on Smart Grid*, vol. 5, no. 4, pp. 1584–1591, Jul. 2014, https://doi.org/10.1109/TSG.2014.2311465.

[26] A. Albaker, A. Majzoobi, G. Zhao, J. Zhang, and A. Khodaei, "Privacy-preserving optimal scheduling of integrated microgrids," *Electric Power Systems Research*, vol. 163, pp. 164–173, Oct. 2018, https://doi.org/10.1016/j.epsr.2018.06.007.

[27] Y. Li, Z. Yang, G. Li, D. Zhao, and W. Tian, "Optimal Scheduling of an Isolated Microgrid With Battery Storage Considering Load and Renewable Generation Uncertainties," *IEEE Transactions on Industrial Electronics*, vol. 66, no. 2, pp. 1565–1575, Oct. 2019, https://doi.org/10.1109/TIE.2018.2840498.

[28] G. Liu, M. Starke, B. Xiao, X. Zhang, and K. Tomsovic, "Microgrid optimal scheduling with chance-constrained islanding capability," *Electric Power Systems Research*, vol. 145, pp. 197–206, Apr. 2017, https://doi.org/10.1016/j.epsr.2017.01.014.

[29] G. Carpinelli, F. Mottola, D. Proto, and P. Varilone, "Minimizing unbalances in low-voltage microgrids: Optimal scheduling of distributed resources," *Applied Energy*, vol. 191, pp. 170–182, Apr. 2017, https://doi.org/10.1016/j.apenergy.2017.01.057.

[30] Y. Li, R. Wang, and Z. Yang, "Optimal Scheduling of Isolated Microgrids Using Automated Reinforcement Learning-Based Multi-Period Forecasting," *IEEE Transactions on Sustainable Energy*, vol. 13, no. 1, pp. 159–169, Jan. 2022, https://doi.org/10.1109/TSTE.2021.3105529.

[31] L. Luo *et al.*, "Optimal scheduling of a renewable based microgrid considering photovoltaic system and battery energy storage under uncertainty," *Journal of Energy Storage*, vol. 28, Apr. 2020, Art. no. 101306, https://doi.org/10.1016/j.est.2020.101306.

[32] *Estimating the Value of Lost Load*. Austin TX, USA: ERCOT, 2013.

[33] "IBM CPLEX — AMPL Resources," *AMPL Development.* https://dev.ampl.com/solvers/cplex/index.html.

AUTHORS PROFILE

Abdullah Albaker received his M.S. and Ph.D. degrees in electrical engineering, specializing in electric power engineering, from the University of Denver, Denver, CO, USA, in 2014 and 2018, respectively. He is currently an Assistant Professor of Electrical Engineering at the University of Ha'il, Ha'il, Saudi Arabia. His research interests include microgrid planning and operation, renewable energy and distributed generation, power system economics and reliability, smart electricity grids optimization, and machine learning.